

## Refractive Index, Temperature and Pressure of Elliptical Plasmonic Waveguide Resonator

Bahram Dehghan<sup>1</sup>; Mojtaba Sadeghi<sup>2\*</sup>; Zahra Adelpour<sup>3</sup>

<sup>1</sup>Department of Electrical Engineering, Shiraz Branch, Islamic Azad University, Shiraz, Iran.

<sup>2\*</sup>Department of Electrical Engineering, Shiraz Branch, Islamic Azad University, Shiraz, Iran.

<sup>2\*</sup>Sadeghi@iaushiraz.ac.ir

<sup>3</sup>Department of Electrical Engineering, Shiraz Branch, Islamic Azad University, Shiraz, Iran.

### Abstract

*This paper proposes the elliptical-shaped based on two-dimensional Metal-Insulator-Metal (MIM) plasmonic waveguide configuration with the sensor characteristics simulated by Finite-Element-Method (FEM). Temperature, refractive index, and pressure are evaluated in the structure by considering the transmission spectrum. As the temperature and refractive index increase, the corresponding curves shift to the right wavelengths. Simulation results show that resonant wavelength of nanocavity shifts to lower wavelength with increasing the pressure. It can be seen that the resonance curves between 1300nm to 1400nm are sharper than the other wavelengths in this structure. The sensitivity and the Figure of Merit (FOM) can be evaluated by considering the mentioned equations. The proposed structure could be applied to develop resonator applications with high sensitivity and tunable response.*

**Key-words:** Temperature, Pressure, Plasmonic, Waveguide.

### 1. Introduction

Surface plasmon polaritons (SPPs) are electromagnetic waves that propagate at the interface between a metal and a dielectric [1]. Some of the promising applications of SPPs are found in gain medium, lasers, amplifiers [2], and sensors [3]. Plasmonic structures are attractive for the future of all-optical devices [4], such as Dielectric-Metal-Dielectric (DMD) [5], resonator structure [6], hybrid plasmonic waveguide [7], Metal-Insulator-Metal (MIM) [8] and etc. Among all suggested structures, optical sensors have been developed to measure a wide variety of parameters so far. Some of the applications of optical sensors are plasmonic sensors which are based on the pressure sensor [9,10],

biosensor [11], refractive index and temperature sensor [12] and etc. One of the most fascinating features of MIM waveguides is the construction of optical sensors by elliptical-shaped plasmonic waveguides [13, 14]. A major advantage of MIM waveguides is better confinement of light with a suitable propagation length for surface plasmon polaritons (SPPs) [15]. Increasing environmental refractive index induces dip position of the transmission spectrum shift towards longer wavelength [12]. Moreover, this scenario exists for temperature and dip minimum of the transmission spectrum.

In this paper, elliptical MIM plasmonic waveguide configuration is presented. Refractive index, temperature, and pressure sensing characteristics investigated in the structure.

The geometry of the configuration and theory are surveyed in Section 2. The results are offered in Section 3 in which the performance of the configuration with refractive index, temperature, and pressure are fully surveyed. Section 4 contains the conclusion part.

The proposed structure has potential advantages such as compact, low cost, and capability for multi-sensing applications.

## 2. Structure and Theory

The MIM plasmonic waveguide geometry is presented in Fig. 1. The blue and gray parts illustrate silver and silica, respectively. The physical parameters  $W$  and  $t$  are the width and port entrance thickness of the MIM waveguide, respectively. Also,  $h_1$  and  $h_2$  parameters are shown in Fig. 1. The specified values of parameters are shown in Table 1. In this analysis, at the wavelength 1550nm, the refractive index of SiO<sub>2</sub> is 1.45. The transmittance in terms of wavelength is calculated by applying a commercial FEM, i.e. COMSOL multiphysics.

In the MIM plasmonic waveguide, the relative permittivity is defined by the Drude model [9, 15].

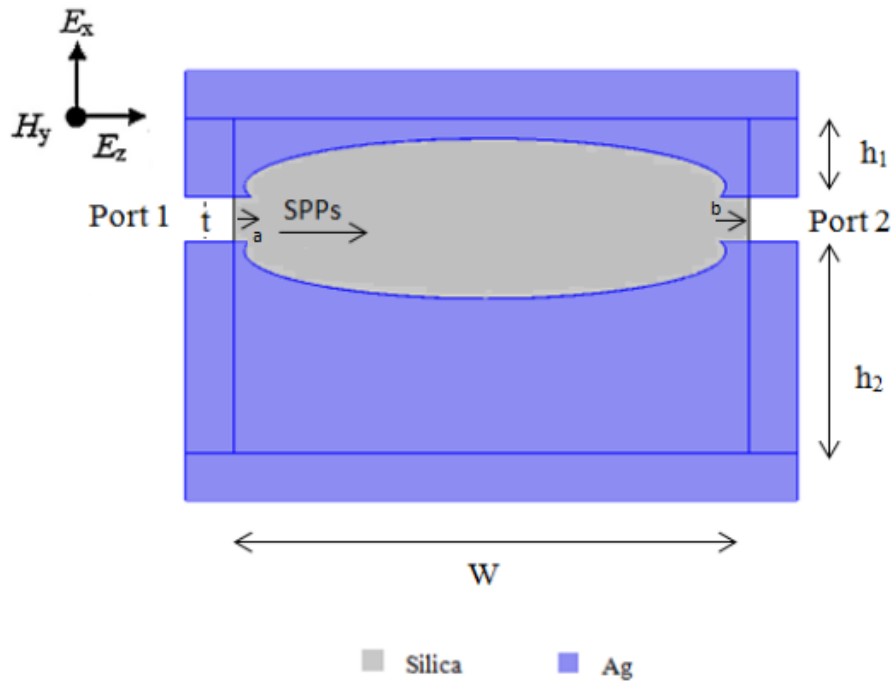
$$\epsilon_m(\omega) = \epsilon_\infty - \frac{\omega_p^2}{\omega^2 + i\gamma\omega} \quad (1)$$

where  $\epsilon_\infty = 3.7$  is the relative permittivity at infinite frequency. Also,  $\omega_p = 9.17\text{eV}$  and  $\gamma = 18\text{meV}$  are the frequency of the plasma oscillations and damping frequency, respectively.

Table 1 – The Values of the Physical Parameters in Fig. 1.

<b>t</b>	<b>h<sub>1</sub></b>	<b>h<sub>2</sub></b>	<b>W</b>	<b>a</b>	<b>b</b>
950nm	1.64μm	4.4μm	10.73μm	0.33μm	0.6μm

Figure 1 - MIM Plasmonic Waveguide Geometry with Perfectly Matched Layers (PML) Representation



The dispersion of primary mode is defined as follows [19]:

$$\frac{\epsilon_i p}{\epsilon_m k} = \frac{1 - e^{kw}}{1 + e^{kw}} \quad (2)$$

$$k = k_0 \sqrt{\left(\frac{\beta_{SPP}}{k_0}\right)^2 - \epsilon_i} , p = k_0 \sqrt{\left(\frac{\beta_{SPP}}{k_0}\right)^2 - \epsilon_m} \quad (3)$$

$$\beta_{SPP} = n_{eff} k_0 = n_{eff} \frac{2\pi}{\lambda} \quad (4)$$

Here,  $\lambda$  is the wavelength in vacuum,  $\epsilon_m$  and  $\epsilon_i$  are metal and dielectric constant, respectively.  $n_{eff}$  is the effective refractive index of MIM waveguide,  $\beta_{SPP}$  is the propagation constant of SPP and  $k_0 = \frac{2\pi}{\lambda}$  is the wavenumber.

By applying the temperature on the structure, the refractive index changes owing to the thermo-optic effect. The refractive index of SiO<sub>2</sub> under temperature is [16]:

$$n = 1.45 + T10^{-5} \quad (5)$$

where T and n are temperature and refractive index, respectively.

The refractive index of SiO<sub>2</sub> under pressure is represented in this study as [10]:

$$n = 1.45 - 0.00965P \quad (6)$$

where the pressure exerted in one direction is indicated by P.

### 3. Results and Discussion

By using FEM and perfectly matched layers (PML), the transmission specifications of the structure are simulated. Based on the results shown in Figure 2a, the transmission spectrum indicates the minimum transmittance at the wavelength of 1371.5 nm is close to zero. The normalized electric field distribution at the wavelength of 1371.5 nm and 1400nm which is shown in Fig. 2b,c clearly indicates the differences between the two introduced wavelengths. Due to elliptical configuration of the structure, the SPPs can be observed in three directions. By changing the refractive index, the transmission curve shifts. The change in displacement of the transmission curve is due to the effects of temperature and pressure.

In the next step, the influence of the refraction index sensitivity is studied. Figure 3a shows that transmission spectrum versus the wavelengths for different refractive index swept from 1.43 to 1.46. As refractive index increases, the transmission spectrum displays a shift towards longer wavelength. The increasing environmental refractive index that induces dip wavelength of the transmission spectrum is exhibited in Fig. 3b. The refractive index sensitivity can be defined as [17]:

$$S = \frac{\Delta\lambda}{\Delta n} \quad (7)$$

where  $\Delta\lambda$  and  $\Delta n$  are the resonant wavelength variation and applied refractive index variation, respectively. The refractive index sensitivity can be obtained 950 nmRIU<sup>-1</sup>. Figure of merit (FoM) is another significant parameter providing an appropriate measurement which means the ratio of sensitivity for wavelength to the bandwidth of resonance can be defined as [6, 18]:

$$FOM = \frac{S}{FWHM} \quad (8)$$

The value of  $166 \text{ RIU}^{-1}$  is calculated in our simulation for FOM. In the next step, the temperature sensing specifications of the configuration are studied. With increasing temperature from  $0$  to  $600^\circ\text{C}$ , the resonant wavelength has a linear shift to a higher wavelength as shown in Fig. 4. The sensitivity for temperature is  $\Delta\lambda/\Delta T$ , this value can be obtained as  $0.01 \text{ nm}/^\circ\text{C}$ .

Finally, the pressure variation of silica is evaluated by the transmission spectrum in the proposed wavelength. There is a linear relationship between the pressure of silica and the wavelength which can be seen in Fig. 5.

Figure 2. a) Transmission Spectrum, The Normalized  $|E|$  Fields of the Structure b) at  $1371.5 \text{ nm}$ , c) at  $1400 \text{ nm}$

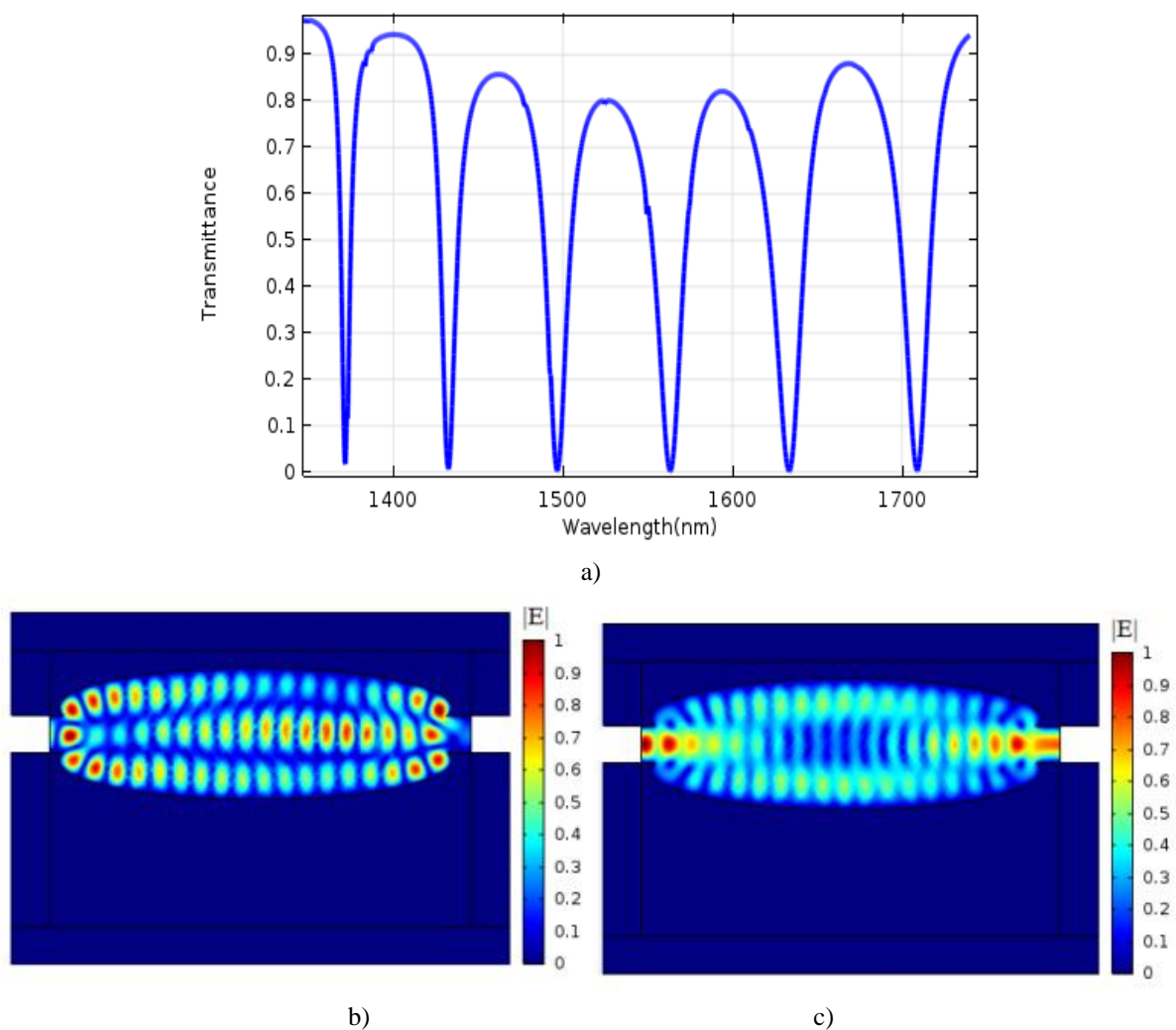


Figure 3. a) The Transmission Spectrum of the Structure with different Refractive Index, b) The Dip Position Versus Refractive Index in the Wavelength Domain from 1340 nm to 1400 nm

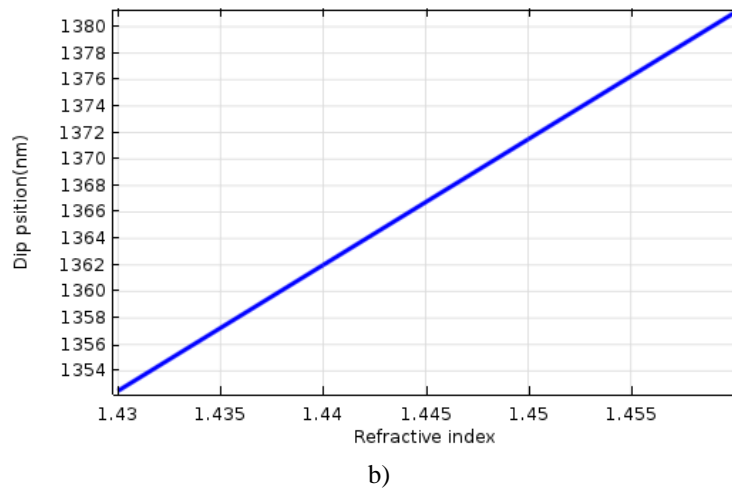
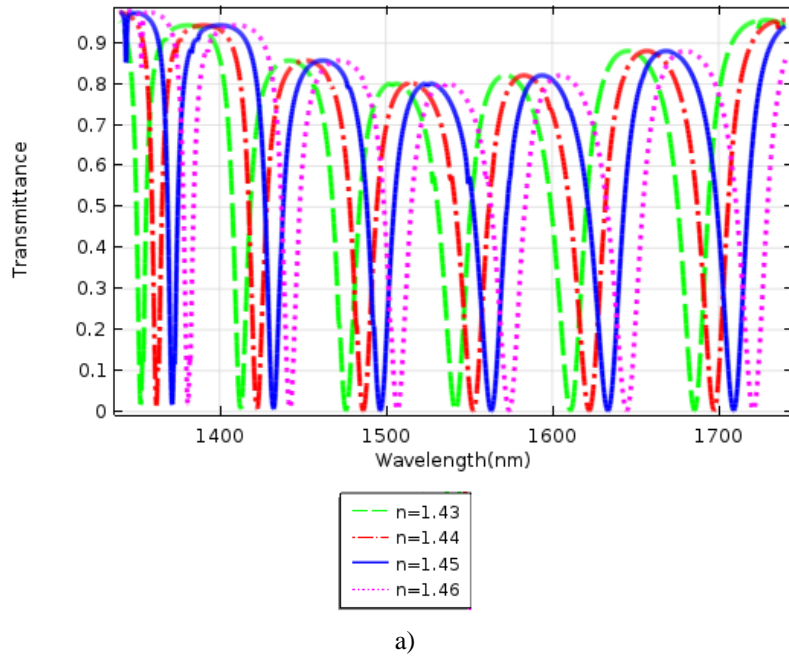


Figure 4 - The Dip Position Versus Temperature in the Wavelength Domain from 1340 nm to 1400 nm

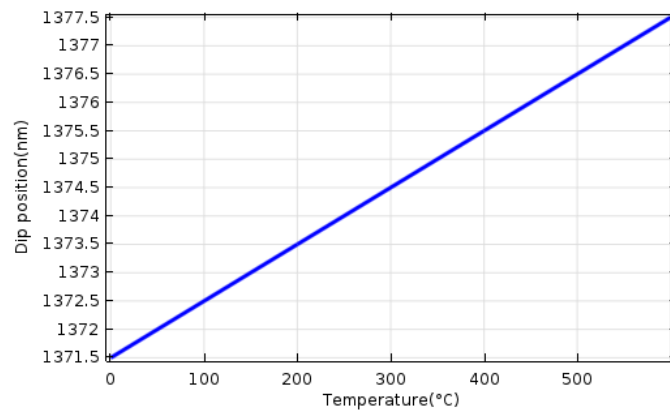
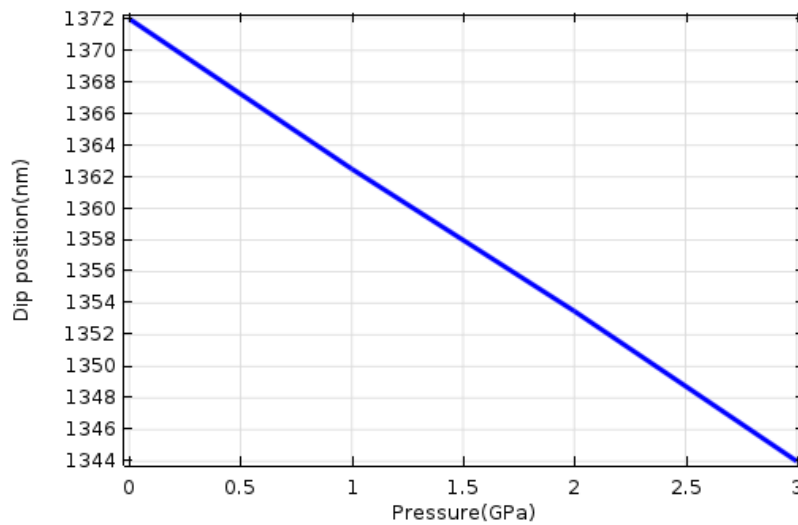


Figure 5 - The Dip Position Versus Pressure in the Wavelength Domain from 1320 nm to 1380 nm



As pressure increases, the transmission spectrum exhibits will be shift towards lower wavelength. The FOM is enhanced at the beginning of the chart because of the sharp and higher transmitted signal. The pressure, sensitivity, and FOM of the first dip position of wavelengths are given in table 2. The table represents a suitable linear relation between the resonance wavelength and the pressure being used. The best FOM and sensitivity, related to 1Gpa.

The results of this study show different sensitivity values at different wavelengths. The designed structure offers a new concept for the compact and highly tunable plasmonic sensor design, such as nanosensor and nanolaser.

Table 2 – The Sensor Components Under Pressure

Pressure(Gpa)	Sensitivity(nm/ Gpa)	FOM(Gpa <sup>-1</sup> )
1	1362.5	252.31
2	676.75	125.32
3	448	82.96

#### 4. Conclusion

In this article, the elliptical plasmonic structure with resonator characteristics was investigated that were affected by temperature, refractive index, and pressure. The proposed plasmonic sensor structure has potential applications in tunable multi-sensing and nanoscale industrial sensing. This work can play an important role in improving the performance of optical circuits.

## References

- Maier, S.A. (2007). *Plasmonics: fundamentals and applications*. Springer Science & Business Media.
- Luo, X., & Yan, L. (2012). Surface plasmon polaritons and its applications. *IEEE Photonics Journal*, 4(2), 590-595.
- Marini, A., Conforti, M., Della Valle, G., Lee, H.W., Tran, T.X., Chang, W., & Biancalana, F. (2013). Ultrafast nonlinear dynamics of surface plasmon polaritons in gold nanowires due to the intrinsic nonlinearity of metals. *New Journal of Physics*, 15(1), 013033.
- Ouahab, I., & Naoum, R. (2016). A novel all optical 4× 2 encoder switch based on photonic crystal ring resonators. *Optik*, 127(19), 7835-7841.
- Kostrobyi, P., Poliovyi, V., Pavlysh, V., & Nevinskyi, D. (2016). Plasmon-polariton waves in the structures “dielectric-metal-dielectric”: Experiment and modeling. *In XIth International Scientific and Technical Conference Computer Sciences and Information Technologies (CSIT)*, 208-211.
- Wu, T., Liu, Y., Yu, Z., Peng, Y., Shu, C., & Ye, H. (2014). The sensing characteristics of plasmonic waveguide with a ring resonator. *Optics express*, 22(7), 7669-7677.
- Dai, D., & He, S. (2009). A silicon-based hybrid plasmonic waveguide with a metal cap for a nano-scale light confinement. *Optics express*, 17(19), 16646-16653.
- Stoja, E., & Frezza, F. (2013). Metal-insulator-metal (mim) plasmonic waveguide based directional couplers operating at telecom wavelengths. *In 6th UK, Europe, China Millimeter Waves and THz Technology Workshop (UCMMT)*, 1-2.
- Duan, G., Lang, P., Wang, L., Yu, L., & Xiao, J. (2016). An optical pressure sensor based on  $\pi$ -shaped surface plasmon polariton resonator. *Modern Physics Letters B*, 30(21), 1650284.
- Dehghan, B., Sadeghi, M., & Adelpour, Z. (2019). The optical characteristics of the defected plasmonic waveguide under pressure. *Optik*, 184, 44-49.
- Rohde, F., & Porcar, R. (2011). A localized surface plasmon sensor for early cancer detection. *In International Workshop on Biophotonics*, 1-3.
- Kong, Y., Qiu, P., Wei, Q., Quan, W., Wang, S., & Qian, W. (2016). Refractive index and temperature nanosensor with plasmonic waveguide system. *Optics Communications*, 371, 132-137.
- Teng, D., Cao, Q., Li, S., & Gao, H. (2014). Tapered dual elliptical plasmon waveguides as highly efficient terahertz connectors between approximate plate waveguides and two-wire waveguides. *JOSA A*, 31(2), 268-273.
- Xue, W., Guo, Y.N., Li, P., & Zhang, W. (2008). Propagation properties of a surface plasmonic waveguide with double elliptical air cores. *Optics express*, 16(14), 10710-10720.
- Sun, L., Wang, J., Wang, Y., Liu, H., Liu, C., & Gao, S. (2015). Electromagnetically induced transparency of double-groove shaped plasmonic waveguide. *Optik*, 126(20), 2596-2599.
- Revathi, S., Inabathini, S.R., & Pal, J. (2015). Pressure and temperature sensor based on a dual core photonic quasi-crystal fiber. *Optik*, 126(22), 3395-3399.
- Ayoub, A.B., & Swillam, M.A. (2017). High performance optical systems using MIM based plasmonic structures. *Journal of Physics Communications*, 1(3), 035007.

Chen, Z., Zhao, X., Lin, C., Chen, S., Yin, L., & Ding, Y. (2016). Figure of merit enhancement of surface plasmon resonance sensors using absentee layer. *Applied optics*, 55(25), 6832-6835.

Zhang, Z., Yang, J., Xu, H., Xu, S., Han, Y., He, X., & Xie, W. (2019). A plasmonic ellipse resonator possessing hybrid modes for ultracompact chipscale application. *Physica Scripta*, 94(12), 125511.

<http://doi.org/10.1088/1402-4896/ab4677>